Journal of the Ceramic Society of Japan 127 [10] 669-677 2019
DOI http://doi.org/10.2109/jcersj2.19081

JCS-Japan

FULL PAPER

Fabrication of bioactive titanium and its alloys by combination of doubled sandblasting process and alkaline simulated body fluid treatment

Takeshi YABUTSUKA[1,†], Hiroshi MIZUNO[1] and Shigeomi TAKAI[1]

[1]Graduate School of Energy Science, Kyoto University, Yoshida-honmachi, Sakyo-ku, Kyoto 606–8501, Japan

In this study, we aimed to improve apatite-forming ability of titanium (Ti) and its alloys, Ti–15Mo–5Zr–3Al, Ti–12Ta–9Nb–6Zr–3V–O, Ti–6Al–4V, and Ti–22V–4Al. The surfaces of Ti and its alloys were treated by the doubled sandblasting process using ceramic grinding particles with 14.0 and 3.0 μm for average particle size. The Ti and its alloys were immersed in the alkaline simulated body fluid (SBF) which was adjusted at higher pH than that in the physiological SBF and were heated in the alkaline SBF by electromagnetic induction. By this treatment, apatite nucleation was promoted near the surface of the substrates and apatite nuclei were precipitated in the pores of the substrates. By immersing in the physiological SBF to test apatite-forming ability, hydroxyapatite was covered the entire surfaces of the Ti and its alloys within 1 day and high apatite-forming ability was shown. The doubled sandblasting process firstly using larger grinding particles and secondly using smaller ones was most effective to increase the surface roughness of the substrates. Average adhesive strength of the hydroxyapatite layer formed in the physiological SBF increased, which depended on the increase of the surface roughness. These results indicated that sandblasting condition was an important factor to improve mechanical interlocking effect related to the increase of the surface roughness and that the doubled sandblasting process had a possibility to be one of the candidates of the treatment to solve this problem.
©2019 The Ceramic Society of Japan. All rights reserved.

Key-words : Titanium, Titanium alloys, Apatite nucleation, Alkaline SBF treatment, Doubled sandblasting process

[Received April 15, 2019; Accepted August 3, 2019]

1. Introduction

Titanium (Ti) and its alloys are one of the main biomedical metallic materials in orthopedics and dentistry together with stainless steels and cobalt–chromium (Co–Cr) alloys and are widely in clinical use because of their good mechanical properties, corrosion resistance and biocompatibility. It was reported that Ti and its alloys can adhere directly to living bone when they are implanted in the body for a long time.[3] However, their bioactivity, that is, the properties that the materials implanted in bone defects spontaneously form hydroxyapatite layer on their surfaces and bond to living bone through the layer, is lower than that of bioactive ceramics such as Bioglass®[1] and glass ceramic A-W®.[2] In order to utilize Ti and its alloys as cementless bone substitutes, it is necessary to improve their osteoconductivity largely.

Various surface modification techniques for Ti and its alloys have been studied to improve their osteoconductivity and adhesion property with bone tissue. Among them, formation of bioactive ceramic films has become their mainstream. As representative conventional methods, sputtering method,[4] plasma spray method,[5] sol–gel method,[6] sodium hydroxide (NaOH) solution-heat treatment[7–9] and so on are mentioned. In the sputtering and plasma spray, however, large expensive equipment is required. In sol–gel method, strictly accurate adjustment of atmosphere is required for suppressing hydrolysis of reaction solution. In addition, objective substrates were needed to be exposed to high temperatures in most of these conventional methods. It was reported that mechanical properties of Ti and its alloys were strongly affected by heat treatment.[10] In particular, the mechanical properties are significantly changed above 773 K and deviate from the desired properties. Therefore, reduction of the processing temperature in the surface modification processes is important.

In our previous study, we presented the fabrication method of bioactive materials by incorporation of apatite nuclei to bioinert materials.[11,12] When the substrates with fine pores were immersed in the physiological simulated body fluid (SBF)[13] which is an aqueous solution with inorganic ion concentrations nearly equal to those of

† Corresponding author: T. Yabutsuka; E-mail: yabutsuka@energy.kyoto-u.ac.jp
‡ Preface for this article: DOI http://doi.org/10.2109/jcersj2.127.P10-1

©2019 The Ceramic Society of Japan

This is an Open Access article distributed under the terms of the Creative Commons Attribution License (https://creativecommons.org/licenses/by-nd/4.0/), which permits unrestricted use, distribution, and reproduction in any medium, provided the original work is properly cited.

human blood plasma, and the pH value and the temperature was increased, homogeneous nucleation of calcium phosphate was accelerated, and apatite nuclei were formed on the surface and in the pores. In this method, high apatite-forming ability was successfully given to various kinds of bioinert materials such as stainless steel,[14] Co–Cr alloy,[15] and polyetheretherketone[16),17] even though the original substrates were completely bioinert. In the previous studies, in addition, we tried to obtain fine pores with complicated shape by the doubled sandblasting process using different sizes of grinding particles on metallic and polymeric materials.[18] When thus-treated substrates were treated with the above alkaline SBF treatment, hydroxyapatite layer formed in the physiological SBF showed higher adhesive strength in comparison with the case of the single sandblasting process using one size of grinding particles by superior mechanical interlocking effects.[14),15),18]

In this study, we aimed to impart high apatite-forming ability to Ti, Ti–15Mo–5Zr–3Al, Ti–12Ta–9Nb–6Zr–3Al–O, Ti–6Al–4V and Ti–22V–4Al by applying above bioactivity treatment. Ti–6Al–4V is ($\alpha + \beta$)-type Ti alloy and most frequently used as a biomaterial because its mechanical toughness is larger than that of pure Ti.[3] Due to the problem that Ti–6Al–4V contains cytotoxic vanadium and its elastic modulus is relatively higher compared with that of cortical bone, development of other-types of Ti alloys has been promoted. Ti–15Mo–5Zr–3Al is β-type Ti alloy which does not contain vanadium. Although having higher strength than Ti–6Al–4V, it has lower elastic modulus and is currently used as a vanadium-free orthopedic implant material.[19] Similarly, Ti–12Ta–9Nb–6Zr–3Al–O has been developed as Ti alloy with high strength and low modulus. This alloy has not only biocompatibility but also superelasticity that exhibits non-linear elastic behavior, that is, Hooke's law does not hold in this alloy. From this reason, application to biomedical materials has been carried out recently.[20] Ti–22V–4Al is one of the most typical β-type Ti alloy in industrial fields and has higher strength and elasticity than those of pure Ti.[21] Although medical application is not performed because it contains a large amount of vanadium, we also used it as a specimen in this study because of its characteristic mechanical properties.

In this study, we researched the fabrication techniques for bioactive Ti, Ti–15Mo–5Zr–3Al, Ti–12Ta–9Nb–6Zr–3Al–O, Ti–6Al–4V and Ti–22V–4Al with combination of the doubled sandblasting process and the alkaline SBF treatment. Firstly, we formed pores on the surface of the substrates by the sandblasting using various combination of the grinding ceramic particles focusing on their particle size. Secondly, we conducted the alkaline SBF treatment to the Ti and its alloys to enrich their apatite-forming ability. Apatite-forming ability of thus treated Ti-based metals was evaluated by immersing in the physiological SBF and observing hydroxyapatite formation on their surfaces. Finally, relationship between the sandblasting conditions, surface roughness and adhesive strength of the formed hydroxyapatite layer was evaluated.

2. Experimental procedures

2.1 Substrates

We used commercially available pure Ti plates (15 × 10 × 2 mm^3, Kobe Steel, Ltd., Kobe, Japan), Ti–15Mo–5Zr–3Al (15 × 10 × 3 mm^3, Kobe Steel, Ltd., Kobe, Japan), Ti–12Ta–9Nb–6Zr–3V–O plates (20 × 10 × 1 mm^3, NISHIMURA CO., LTD, Sabae, Fukui, Japan), Ti–6Al–4V (20 × 10 × 1 mm^3, NISHIMURA CO., LTD) and Ti–22V–4Al (15 × 10 × 1 mm^3, FUTA-Q, Ltd., Kyoto, Japan) and Ti dental implant (φ3.5 mm × 11 mm^3, 2.0 mm well, Bicon Dental Implants, Boston, MA) were used as substrates.

2.2 Doubled sandblasting process

The surfaces of the Ti, Ti–15Mo–5Zr–3Al, Ti–12Ta–9Nb–6Zr–3V–O, Ti–6Al–4V, and Ti–22V–4Al were sandblasted twice with grinding particles with both 14.0 and 3.0 μm in average diameter, that is, we firstly sandblasted the substrates using the 14.0 μm ceramics particles and secondly the 3.0 μm ones. For Ti, Ti–15Mo–5Zr–3Al and Ti–12Ta–9Nb–6Zr–3V–O, we used silicon carbide particles as the grinding particles because of their high Vickers hardness (23 GPa). For Ti–6Al–4V and Ti–22V–4Al, we used alumina grinding particles from a viewpoint of the utilization in biomedical or dental application although Vickers hardness (15 GPa) was lower than that of silicon carbide. We applied discharge pressure at 0.85 MPa using an oil-free scroll compressor (SRL-3.7DMA5, Hitachi Industrial Equipment Systems Co., Ltd., Tokyo, Japan) in the above sandblasting procedure. After that, each plate was washed with acetone using an ultrasonic cleaner for 90 min and airdried.

The surfaces of the substrates were analyzed using field emission scanning electron microscope (SEM; SU6600, Hitachi High-Technologies Corporation, Tokyo, Japan) and energy dispersive X-ray spectrometer (EDS; Xflash® 5010, Bruker AXS Inc., Fitchburg, WI). Before the SEM and EDS observation, gold was coated on the plates by sputtering method. Changes in surface roughness of the surface of the substrates were analyzed by three-dimensional measuring laser microscope (LEXT OLS4000-SAT, Olympus Corporation, Tokyo, Japan). The surface roughness was calculated by the method certified as ISO 25178.

In order to compare an effect of the combination of size of grinding particles, we conducted the doubled or single sandblasting process to Ti–15Mo–5Zr–3Al using the silicon carbide grinding particles with particle size as shown in **Table 1**. In the condition codes in Table 1, 'N' means that the sandblasting was not conducted. '14' or '3' means that the sandblasting using the 14.0 or 3 μm grinding particles was conducted in the first or second sandblasting. Each sample was washed with acetone using an ultrasonic cleaner and airdried after the sandblasting.

2.3 Preparation of physiological SBF

The physiological SBF (Na^+; 142.0, K^+; 5.0, Mg^{2+}; 1.5, Ca^{2+}; 2.5, Cl^-; 147.8, HCO_3^-; 4.2, HPO_4^{2-}; 1.0,

SO_4^{2-}; 0.5 mmol·dm^{-3}) was prepared by the method certified in ISO 23317. First, we dissolved the certified amount of reagent-grade NaCl, $NaHCO_3$, KCl, $K_2HPO_4 \cdot 3H_2O$, $MgCl_2 \cdot 6H_2O$, 1 mol·dm^{-3} HCl, $CaCl_2$, Na_2SO_4 and tris(hydroxymethyl)aminomethane in ultrapure water in this order. Finally, we adjusted pH value at 7.40 at 36.5°C using 1 mol·dm^{-3} HCl and volume of the solution using ultrapure water and a measuring flask.

2.4 Alkaline SBF treatment

The alkaline SBF was prepared by raising pH value of the physiological SBF from 7.40 to 8.10 or 8.20 at 36.5°C by dissolving tris(hydroxymethyl)aminomethane. In the alkaline SBF treatment, the alkaline SBF at pH = 8.10 was used for Ti, Ti–15Mo–5Zr–3Al and Ti–12Ta–9Nb–6Zr–3V–O, and that at pH = 8.20 was used for Ti–6Al–4V and Ti–22V–4Al because their reproducibility in the case of pH = 8.10 was relatively lower for these alloys. The substrates were immersed in the alkaline SBF in the rubber bags and the solution was pressed at 200 MPa for 60 min using cold isostatic pressing machine (CIP-SI, Kobe Steel, Ltd., Kobe, Japan) to penetrate the solution in the pores of the substrate. Next, the plates were heated for 180 min by electromagnetic induction heating equipment (KZ-KM22B, Panasonic Corporation, Osaka, Japan) at 3 kW of output power during immersed in the alkaline SBF. By this treatment, apatite nuclei were precipitated in the pores of the substrates. After the treatment, the substrates were washed with ultrapure water and airdried. The surfaces of the substrates were analyzed by thin film X-ray diffraction instrumentation (TF-XRD; Rint 2500, Rigaku Corporation, Tokyo, Japan). The TF-XRD measurements were conducted using Cu-Kα radiation at 50 kV of tube voltage and 300 mA of tube current.

Table 1. Combination of size of grinding particles in the sandblasting processes

Condition code	Particle size in 1st sandblasting	Particle size in 2nd sandblasting
N	—	—
14-N	14.0 μm	—
3-N	3.0 μm	—
3-14	3.0 μm	14.0 μm
3-3	3.0 μm	3.0 μm
14-3	14.0 μm	3.0 μm

2.5 Test of apatite-forming ability

In order to test apatite-forming ability of the substrate treated with alkaline SBF in the previous section, each substrate was immersed in the physiological SBF for 1 day, 3 days, 7 days and 14 days. After immersing in SBF, the substrates were washed with ultrapure water and airdried. The surfaces of the substrates were analyzed by the TF-XRD, SEM and EDS.

2.6 Test of adhesive strength of hydroxyapatite layer formed in the physiological SBF

Adhesive strength of hydroxyapatite layer formed on the alkaline SBF-treated substrates by immersing in the physiological SBF for 14 days was measured by a modified ASTM C-633.[8),22)–24)] A couple of stainless jigs (10 × 10 mm^2) were adhered to the surface of the substrate using epoxy-type glue (Araldite®, Nichiban Co., Ltd., Tokyo, Japan). Tensile load was applied at 1 mm·min^{-1} using universal testing machine (Model AGS-H Autograph, Shimadzu Corporation, Kyoto, Japan) until fracture between the hydroxyapatite layer and the substrate were occurred.

3. Results

Figure 1 shows the average surface roughness of the Ti, Ti–15Mo–5Zr–3Al, Ti–12Ta–9Nb–6Zr–3V–O, Ti–6Al–4V and Ti–22V–4Al plates after the doubled sandblasting treatment using 14.0 μm first grinding particles and 3.0 μm subsequent ones. For the reference, those of the untreated plates are also shown. S_a is an arithmetic average roughness and S_z is a maximum height of irregularities. It can be seen that the surface roughness was clearly increased by conducting the above doubled sandblasting process. Significant difference of the average values among all the types of plates was not observed.

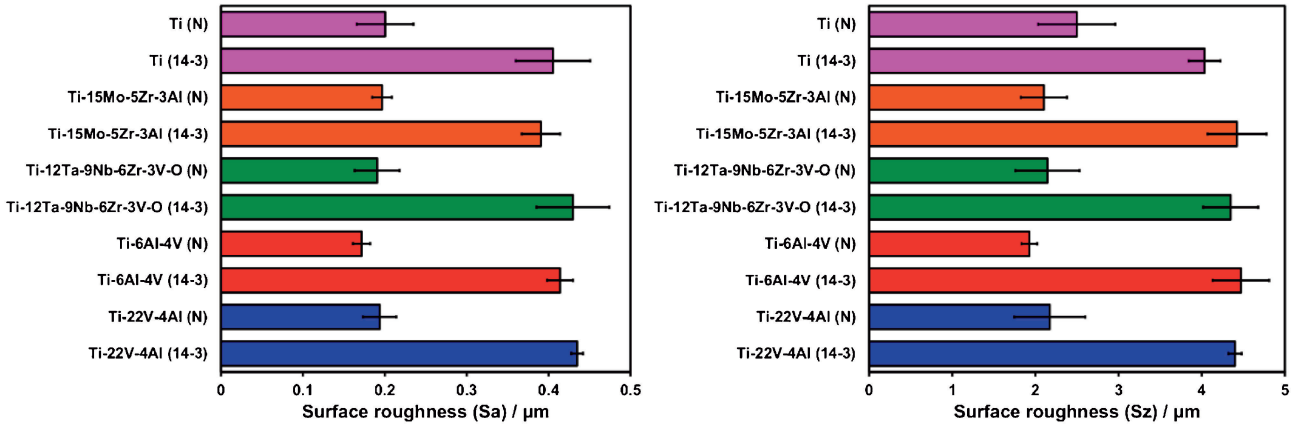

Fig. 1. Average surface roughness (S_a and S_z) of the Ti, Ti–15Mo–5Zr–3Al, Ti–12Ta–9Nb–6Zr–3V–O, Ti–6Al–4V and Ti–22V–4Al plates with and without the doubled sandblasting treatment using 14.0 μm first grinding particles and 3.0 μm subsequent ones.

Figure 2 shows the surfaces of the Ti, Ti–15Mo–5Zr–3Al, Ti–12Ta–9Nb–6Zr–3V–O, Ti–6Al–4V and Ti–22V–4Al plates after the doubled sandblasting treatment using 14.0 µm first grinding particles and 3.0 µm subsequent ones and followed by immersing in the physiological SBF for 14 days. Hydroxyapatite formation was not observed for each plate regardless of the types of the Ti alloys. This result indicates that Ti and its alloys did not show apatite-forming ability only treated with sandblasting. In addition, the peak of Si was detected in Ti, Ti–15Mo–5Zr–3Al, and Ti–12Ta–9Nb–6Zr–3V–O just after the alkaline SBF treatment. This result indicates that the contamination of silicon carbide grinding particles remaining on surface of the Ti alloys. Also, in the case of Ti–6Al–4V and Ti–22V–4Al, the alumina grinding particles might exist on these samples because the peak of Al clearly appeared as well as those of Ti.

Figure 3 shows the TF-XRD patterns of the surfaces of the alkaline SBF-treated Ti, Ti–15Mo–5Zr–3Al, Ti–12Ta–9Nb–6Zr–3V–O, Ti–6Al–4V and Ti–22V–4Al plates after the immersion in the physiological SBF for 0 day (just after the alkaline SBF treatment), 1 day, 3 days and 7 days. Just after the alkaline SBF treatment, diffraction peaks of hydroxyapatite were not detected for all the types of plates. After immersing in the physiological SBF for 1 day, diffraction peaks of hydroxyapatite were slightly detected for all the types of plates. After 3 days, such diffraction peaks were intensified in comparison with those after 1 day. After 7 days, intensity and number of the diffraction peaks were further increased. These results indicated that apatite formation was induced in the physiological SBF within 1 day regardless of elemental compositions of the Ti alloys. In addition, peak intensity of hydroxyapatite after the immersion for 1 day for Ti–6Al–4V and Ti–22V–4Al was higher than the other-types of alloys. This reason might be the difference of pH value of the alkaline SBF.

Figure 4 shows the SEM images of the surface of the Ti, Ti–15Mo–5Zr–3Al, Ti–12Ta–9Nb–6Zr–3V–O, Ti–6Al–4V and Ti–22V–4Al plates just after the alkaline SBF treatment and after immersing in the physiological

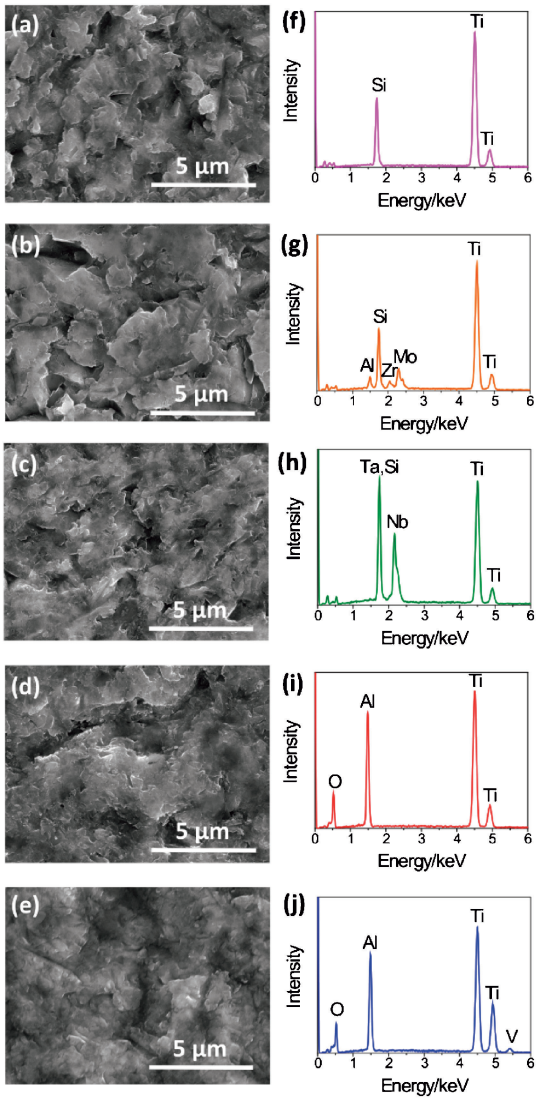

Fig. 2. (a–e) SEM images and (f–j) EDS profiles of the surface of the (a, f) Ti, (b, g) Ti–15Mo–5Zr–3Al, (c, h) Ti–12Ta–9Nb–6Zr–3V–O, (d, i) Ti–6Al–4V and (e, j) Ti–22V–4Al plates after the doubled sandblasting treatment using 14.0 µm first grinding particles and 3.0 µm subsequent ones and followed by immersing in the physiological SBF for 14 days.

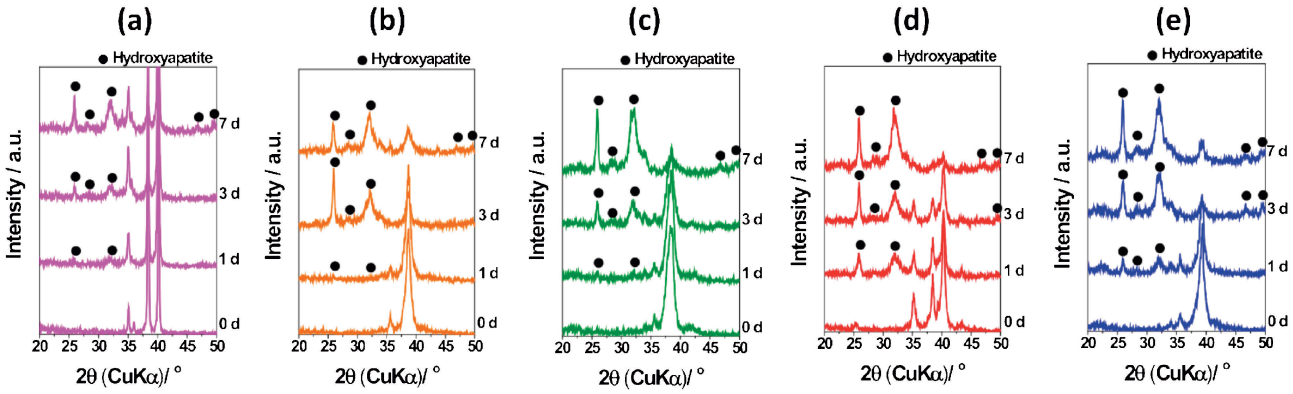

Fig. 3. TF-XRD patterns of the surfaces of the alkaline SBF-treated (a) Ti, (b) Ti–15Mo–5Zr–3Al, (c) Ti–12Ta–9Nb–6Zr–3V–O, (d) Ti–6Al–4V and (e) Ti–22V–4Al plates after the immersion in the physiological SBF for 0 day (just after the alkaline SBF treatment), 1 day, 3 days and 7 days.

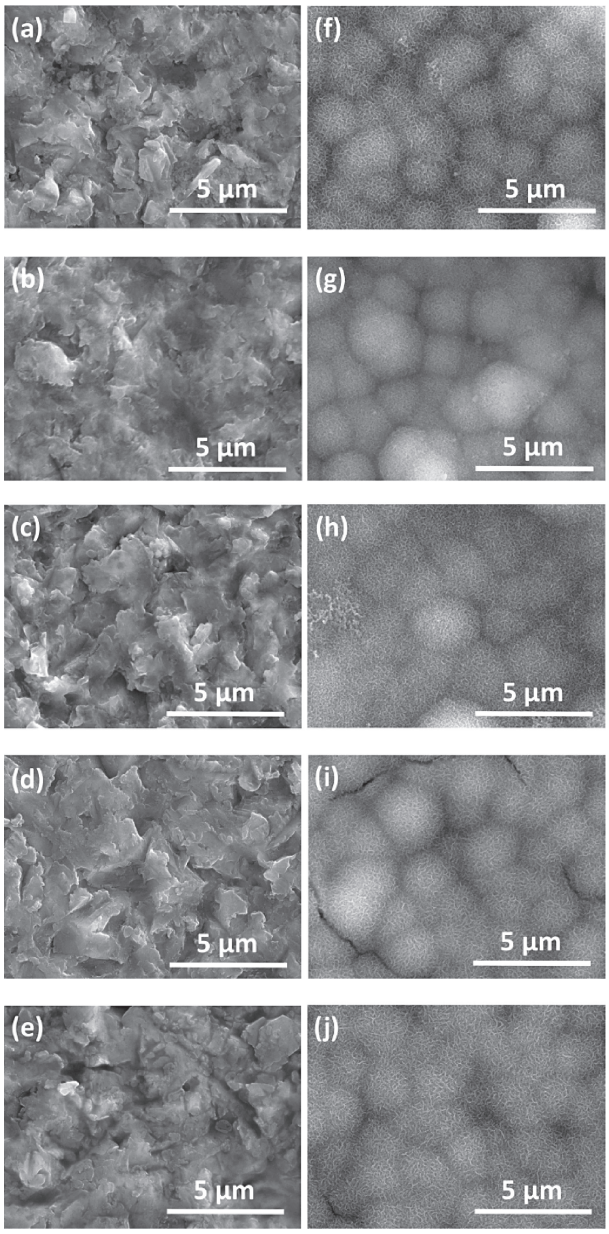

Fig. 4. SEM images of the surface of the (a, f) Ti, (b, g) Ti–15Mo–5Zr–3Al, (c, h) Ti–12Ta–9Nb–6Zr–3V–O, (d, i) Ti–6Al–4V and (e, j) Ti–22V–4Al plates (a–e) just after the alkaline SBF treatment and (f–j) after immersing in the physiological SBF for 1 day.

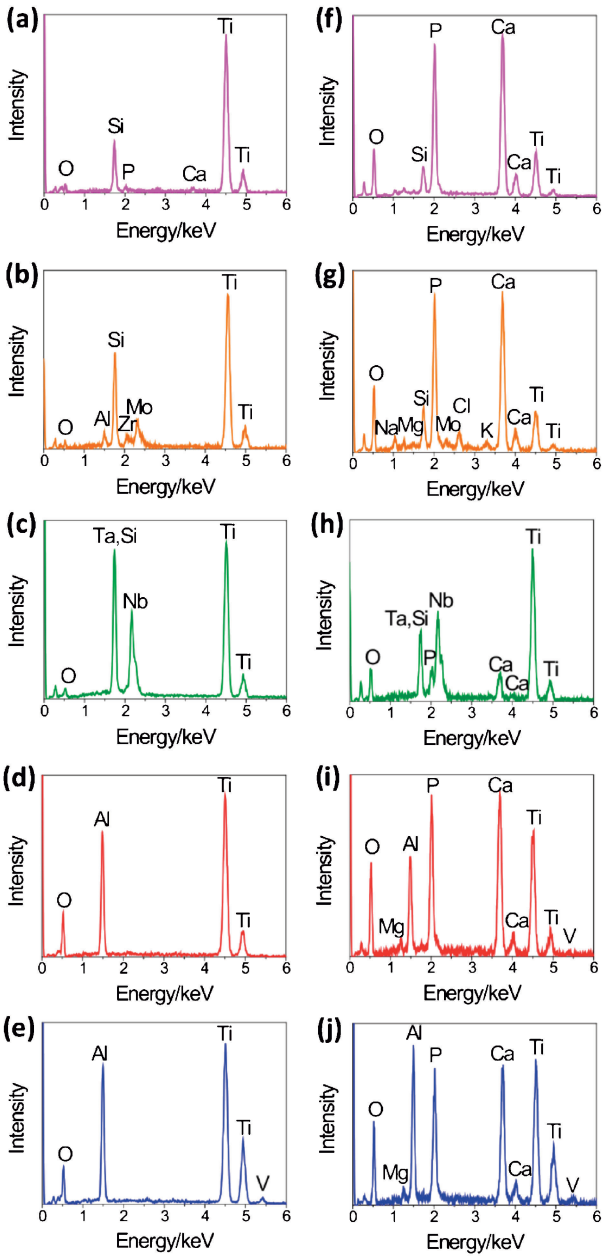

Fig. 5. EDS spectra of the surface of the (a, f) Ti, (b, g) Ti–15Mo–5Zr–3Al, (c, h) Ti–12Ta–9Nb–6Zr–3V–O, (d, i) Ti–6Al–4V and (e, j) Ti–22V–4Al plates (a–e) just after the alkaline SBF treatment and (f–j) after immersing in the physiological SBF for 1 day.

SBF for 1 day. After the alkaline SBF treatment, roughened surfaces obtained by the doubled sandblasting process were observed. Apatite nuclei could not be observed because their size was too small to be observed in SEM level similar to our previous study in which we applied sulfuric acid treatment for pores formation.[25] After immersing in the physiological SBF for 1 day, it can be seen that needle-like crystallites, characteristic to hydroxyapatite formed in SBF, covered their entire surfaces for all the types of plates. These results indicate that induced apatite covered the entire surfaces of all the types of plates in the physiological SBF for 1 day and high apatite-forming ability was given to them.

Figure 5 shows the EDS spectra of the surface of the Ti, Ti–15Mo–5Zr–3Al, Ti–12Ta–9Nb–6Zr–3V–O, Ti–6Al–4V and Ti–22V–4Al plates just after the alkaline SBF treatment and after the immersing in the physiological SBF for 1 day. After the alkaline SBF treatment, peaks of P and Ca were hardly detected except for the Ti. This result indicated that it is difficult to detect apatite nuclei by EDS. After immersing in the physiological SBF for 1 day, it can be seen that peaks of P and Ca, constituents of hydroxyapatite, were clearly observed on all the types of plates. This result indicated that apatite nuclei grew in the physiological SBF.

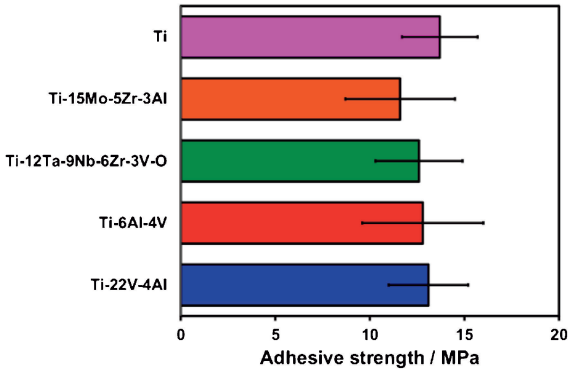

Fig. 6. Average adhesive strength of the hydroxyapatite layer on the surface of the Ti, Ti–15Mo–5Zr–3Al, Ti–12Ta–9Nb–6Zr–3V–O, Ti–6Al–4V and Ti–22V–4Al plates formed by immersing in the physiological SBF for 14 days.

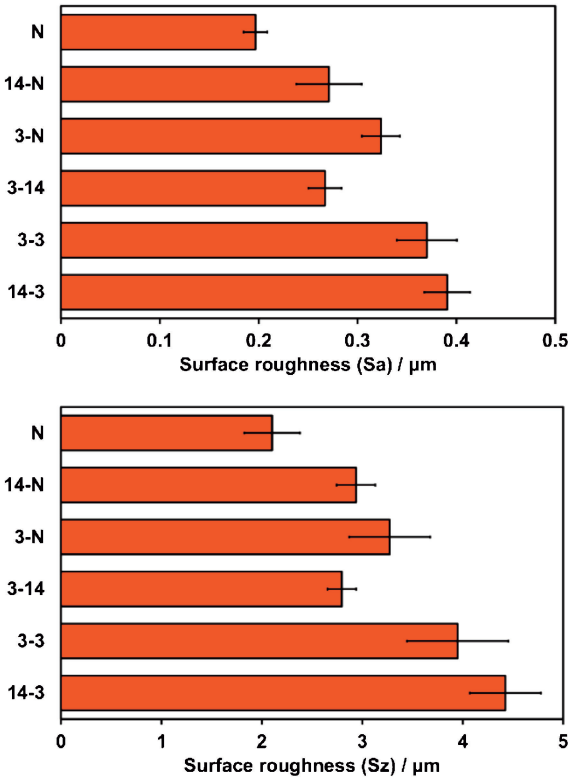

Fig. 7. Average surface roughness (S_a and S_z) of the Ti–15Mo–5Zr–3Al plates treated with the sandblasting condition of N, 14-N, 3-N, 3-14, 3-3 and 14-3 shown in Table 1.

Figure 6 shows the average adhesive strength of the hydroxyapatite layer on the surface of the Ti, Ti–15Mo–5Zr–3Al, Ti–12Ta–9Nb–6Zr–3V–O, Ti–6Al–4V and Ti–22V–4Al plates formed by immersing in the physiological SBF for 14 days. It can be seen that the average adhesive strength showed more than 10 MPa regardless of the elemental composition of the Ti alloys.

Figure 7 shows the average surface roughness of the Ti–15Mo–5Zr–3Al plates treated with the sandblasting condition of 14-N, 3-N, 3-14, 3-3 and 14-3 shown in Table 1. For Sample N, apatite was partially formed on the surface of the substrate, that is, it did not cover the whole surface of the substrate even after soaking in SBF for 14 days. Hence, we could not carry out the evaluation of the adhesive strength. The average value of the surface roughness was in the order of 3-14 ≈ 14-N < 3-N < 3-3 < 14-3. Condition N showed the smallest value. Conditions 3-14 and 14-N, which applied the 14.0 μm particles in the final stage of the sandblasting, showed similar values. In comparison based on the particle size in the single sandblasting, condition 3-N showed larger value than 14-N. In comparison based on a frequency of the sandblasting, Condition 3-3 showed larger value than 3-N. In comparison based on the particle size using the first process in the doubled sandblasting, condition 14-3 showed larger value than 3-3.

Figure 8 shows the SEM images and SEM oblique images of the cross-section of the surfaces of the Ti–15Mo–5Zr–3Al alloy in the sandblasting condition of 14-N, 3-N, 3-14, 3-3 and 14-3 after immersing in the physiological SBF for 14 days. Thickness of the hydroxyapatite layer showed large variability for each specimen. However, it can be seen that range of the thickness of the hydroxyapatite layer was around 50 μm regardless of the sandblasting condition.

Figure 9 shows the average adhesive strength of the hydroxyapatite layer on the Ti–15Mo–5Zr–3Al plates treated with the sandblasting condition of 14-N, 3-N, 3-14, 3-3 and 14-3 formed by immersing in the physiological SBF for 14 days. The average values of the adhesive strength were in the order of 3-14 ≈ 14-N < 3-N < 3-3 < 14-3. This order corresponded to the tendency in the surface roughness. The relationship between the thickness of the apatite layer and its adhesive strength was not clarified.

Figure 10 shows the SEM image and the EDS spectrum of the surfaces of the alkaline SBF-treated Ti dental implant after immersing in the physiological SBF for 1 day. Also, in the case of the commercially available dental implant, hydroxyapatite covered their entire surfaces and peaks of P and Ca, constituents of hydroxyapatite, strongly detected. This result indicates that the alkaline SBF treatment was applicable not only to the plates but also the dental implants in practical use.

4. Discussion

The present study showed that the alkaline SBF treatment was effective to impart high apatite-forming ability to the Ti and its alloys regardless of their elemental composition because the spontaneous formation of hydroxyapatite layer was shown on all the types of substrates in the physiological SBF within 1 day. It is known that most of bioactive ceramics in clinical use show apatite-forming ability in the physiological SBF within 7 days[26] and this is one of the required material properties to bond to living bone. It has been reported that untreated Ti required more than 30 days to induce hydroxyapatite formation in Hank's solution, which is one of the representative different type of SBF.[27] Also, it was reported that the NaOH-heat treated Ti, which is in clinical use as hip joint, induced hydroxy-

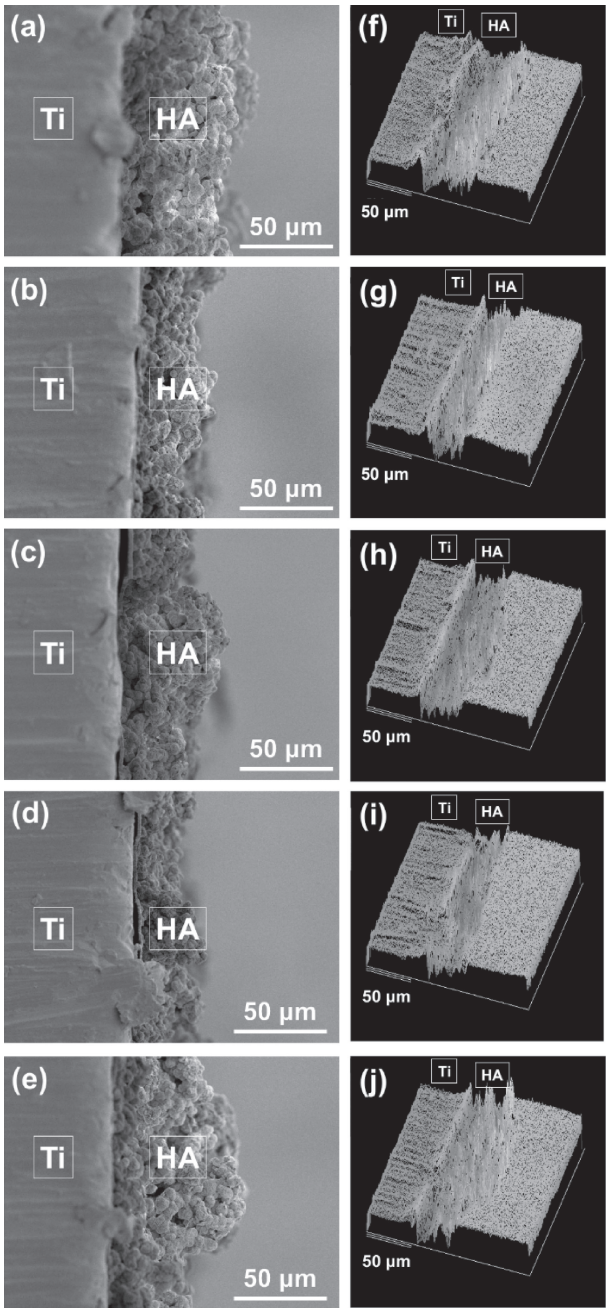

Fig. 8. (a–e) SEM images and (f–j) SEM oblique images of the cross-section of the surfaces of the Ti–15Mo–5Zr–3Al alloy in the sandblasting condition of (a, f) 14-N, (b, g) 3-N, (c, h) 3-14, (d, i) 3-3 and (e, j) 14-3 after immersing in the physiological SBF for 14 days. In this figure, 'Ti' means the Ti–15Mo–5Zr–3Al plate and 'HA' means hydroxyapatite layer.

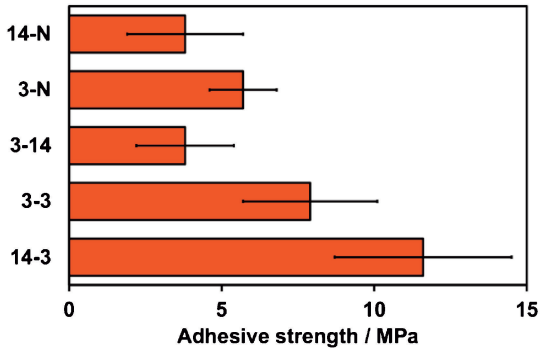

Fig. 9. Average adhesive strength of the hydroxyapatite layer on the Ti–15Mo–5Zr–3Al alloy in the sandblasting condition of 14-N, 3-N, 3-14, 3-3 and 14-3 formed by immersing in the physiological SBF for 14 days.

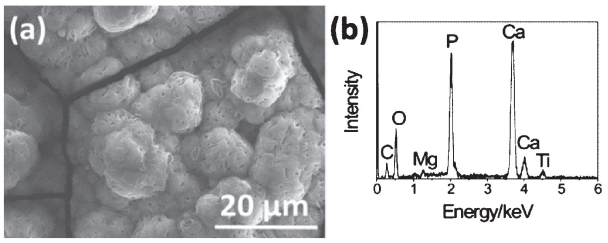

Fig. 10. (a) SEM image and the (b) EDS spectrum of the surfaces of the alkaline SBF-treated Ti dental implant after immersing in the physiological SBF for 1 day.

apatite formation within 1 day in the physiological SBF.[9] Therefore, it is suggested that apatite-forming ability of the Ti and its alloys treated with the alkaline SBF prepared in this study was almost comparative level.

The Ti and its alloys treated with alkaline SBF showed hydroxyapatite formation within 1 day in the physiological SBF. This result suggested that the attached apatite nuclei on the substrate induced hydroxyapatite formation on the entire surface of each substrate and apatite-forming ability of the Ti and its alloys was largely improved. In the case of the stainless steels in our previous study,[14] calcium phosphate film could be observed on the substrates just after the alkaline SBF treatment. It is speculated that such difference between stainless steels and Ti and its alloys was caused by that of heating efficiency derived from a difference of magnetic susceptibility between Fe ($217.6 \times 10^{-6}\,cm^3 \cdot mol^{-1}$) and Ti ($3.19 \times 10^{-6}\,cm^3 \cdot mol^{-1}$).[28]

In Ti–6Al–4V and Ti–22V–4Al, higher pH of alkaline SBF than other-types of Ti alloys was required to improve reproducibility. It is speculated that the existence of vanadium or combination of aluminum and vanadium might inhibit hydroxyapatite formation in SBF.

In addition, this study represents that the particle size and the combination of the grinding particles in the sandblasting process was tightly related to the surface roughness of the substrate and the adhesive strength of hydroxyapatite layer formed in the physiological SBF. From a viewpoint of the size of grinding particles, firstly, applying the 3 μm grinding particles, that is, smaller grinding particles, especially in the final stage in the sandblasting process was available for attainment of larger surface roughness of the Ti alloys and adhesive strength of the hydroxyapatite layer. Secondly, the doubled sandblasting process using the 14 μm grinding particles, that is, larger grinding particles, and subsequent the 3 μm ones, that is, smaller ones, showed larger surface roughness and higher adhesive strength of the hydroxyapatite layer than those of the case of each single sandblasting process. These results

of the adhesive strength are a similar tendency to the doubled sandblasting process to the stainless steel[14] and Co–Cr alloy[15] reported in our previous study. It was revealed that the sandblasting condition which realizes large surface roughness was an important factor for improvement of mechanical interlocking effect between the substrate and the hydroxyapatite. Therefore, the doubled sandblasting process in such combination, which showed the highest surface roughness in this study, has a possibility to be a candidate for the effective surface treatment to attain high adhesive strength of the hydroxyapatite layer formed in living body.

The average adhesive strength apatite layer to the substrates was more than approximately 10 MPa. This value is lower than the NaOH-heat treatment.[7] However, the advantage of our method is to be possible to improve the adhesive strength further by changing the frequency of the sandblasting and the combination of the size of grinding particles. In addition, our method can apply not only Ti-based metals but also other types of bioinert metals such as stainless steels and Co–Cr alloys as reported in our previous studies,[14),15] which was not achieved by the NaOH-heat treatment.[8]

After the sandblasting processes, the grinding particles remained on the surface of the substrate even after the washing by ultrasonication for 90 min. For biomedical application, we think that it is necessary to remove the contamination of these microparticles. However, we think that there is a limitation of only conventional ultrasonication cleaning for solving this problem. This problem might be solved by using water-soluble particles instead of silicon carbide or alumina particles in the sandblasting process.

We acknowledge that there are several limitations in this experiment. First, the apatite nuclei formed on the substrate in the alkaline SBF treatment were hardly observed in the SEM observation. This tendency was similar to the case of the sulfuric acid-treated Ti[25] in our previous studies. In order to clarify this point, we think that other analytical examination with more high precision such as transmission electron microscopy observation is needed. Also, it is considered that amount of apatite nuclei attached on the substrate is related to surface roughness or surface area and these factors may affect the apatite formation in SBF. Hence, we think that quantitative analysis of apatite nuclei such as X-ray photoelectron spectroscopy is also needed in our future study. However, the substrates showed high apatite-forming ability within 1 day irrespective of the kinds of the Ti alloys. From this reason, we think that this fabrication method using alkaline SBF is meaningful for promoting apatite-forming ability of Ti and its alloys. Second point is a relationship between surface condition of Ti and its alloys and the apatite nucleation. In this study, we heated the Ti and its alloys in an aqueous solution using induction heating. Therefore, there is a possibility that surface condition such as the existence of passivation films may be changed by the induction heating and such change may also affect the apatite nucleation in the alkaline SBF. We will examine these points in a future study.

5. Conclusions

The surfaces of Ti, Ti–15Mo–5Zr–3Al, Ti–12Ta–9Nb–6Zr–3V–O, Ti–6Al–4V, and Ti–22V–4Al were sandblasted twice using the 14.0 μm grinding particles and subsequently using the 3.0 μm ones. The Ti and its alloys were immersed in the alkaline SBF and heated by electromagnetic induction. By this treatment, apatite nuclei were precipitated in the pores of the substrates. Thus-treated Ti and its alloys showed apatite-forming ability in a short time. The doubled sandblasting process firstly using larger grinding particles and secondly using smaller ones was most effective to improve adhesion of the hydroxyapatite layer formed in the physiological SBF to the substrates because of its larger surface roughness. The combination of the doubled sandblasting treatment and the alkaline SBF treatment will be contributable to improve adhesion to bone tissue of bioinert or poorly bioactive materials.

Acknowledgment This work was partly supported by Kyoto University Supporting Program for Interaction-based Initiative Team Studies (SPIRITS), Iketani Science and Technology Foundation (ISTF), and LNest Grant from Leave a Nest Co., Ltd.

References

1) L. L. Hench, *J. Biomed. Mater. Res.*, **74**, 1487–1510 (1991).
2) T. Kokubo, M. Shigematsu, Y. Nagashima, M. Tashiro, T. Yamamuro and S. Higashi, *Bull. Inst. Chem. Res. Kyoto Univ.*, **60**, 260–268 (1982).
3) T. Hanawa, *J. Jpn. Inst. Light Met.*, **62**, 285–290 (2012).
4) D. R. Cooley, A. F. Van Dellen, J. O. Burgess and A. S. Windeler, *J. Prosthet. Dent.*, **67**, 93–100 (1992).
5) K. de Groot, R. Geesink, C. P. A. T. Klein and P. Serekia, *J. Biomed. Mater. Res.*, **21**, 1375–1387 (1987).
6) T. Peltola, M. Pätsi, H. Rahiala, I. Kangasniemi and A. Yli-Urpo, *J. Biomed. Mater. Res.*, **41**, 504–510 (1998).
7) H.-M. Kim, F. Miyaji, T. Kokubo and T. Nakamura, *J. Biomed. Mater. Res.*, **32**, 409–417 (1996).
8) H.-M. Kim, F. Miyaji, T. Kokubo and T. Nakamura, *J. Biomed. Mater. Res.*, **38**, 121–127 (1997).
9) S. Yamaguchi, H. Takadama, T. Matsushita, T. Nakamura and T. Kokubo, *J. Ceram. Soc. Jpn.*, **117**, 1126–1130 (2009).
10) M. Ikeda, S. Komatsu, T. Sugimoto and M. Hasegawa, *Mat. Sci. Eng. A-Struct.*, **243**, 140–145 (1998).
11) T. Yao, M. Hibino and T. Yabutsuka, *U.S. Patent* 8512732 (2013).
12) T. Yao, M. Hibino and T. Yabutsuka, *Japanese Patent* 5252399 (2013).
13) T. Kokubo and H. Takadama, *Biomaterials*, **27**, 2907–2915 (2006).
14) T. Yabutsuka, R. Karashima, S. Takai and T. Yao, *Materials*, **11**, 1334 (2018).
15) T. Yabutsuka, H. Mizutani, S. Takai and T. Yao, *Trans. Mater. Res. Soc. Jpn.*, **43**, 143–147 (2018).
16) T. Yabutsuka, K. Fukushima, T. Hiruta, S. Takai and T. Yao, *Mater. Sci. Eng., C*, **81**, 349–358 (2017).

17) T. Yabutsuka, K. Fukushima, T. Hiruta, S. Takai and T. Yao, *J. Biomed. Mater. Res. B*, 106, 2254–2265 (2018).
18) T. Yao and T. Yabutsuka, *Japanese Patent* 6071895 (2017).
19) M. Todai, K. Hagiwara, T. Ishimoto, K. Yamamoto and T. Nakano, *Tetsu To Hagane*, 101, 37–41 (2015).
20) Y. Oda, *Shikwa Gakuho*, 114, 187–197 (2014).
21) S. Fukui, Y. Ohtakara and A. Suzuki, *Denki Seiko*, 4, 303–317 (1986).
22) W. R. Lacefield, "An Introduction to Bioceramics, Second Edition", Ed. by L. L. Hench, Imperial College Press, London (2013) pp. 331–347.
23) T. Miyazaki, H.-M. Kim, T. Kokubo, C. Ohtsuki, K. Kato and T. Nakamura, *J. Mater. Sci.-Mater. M.*, 13, 651–655 (2002).
24) J. A. Juhasz, S. M. Best, M. Kawashita, N. Miyata, T. Kokubo and T. Nakamura, *J. Biomed. Mater. Res.*, 67A, 952–959 (2003).
25) T. Yabutsuka, M. Hibino, T. Yao, K. Tanaka, M. Takemoto, M. Neo and T. Nakamura, *Bioceram. Dev. Appl.*, 1, D110122 (2011).
26) T. Kokubo, "Bioceramics and their clinical applications", Woodhead Publishing Limited, Cambridge (2008).
27) T. Narushima, *Met. Technol. Japan*, 77, 122–127 (2007).
28) The Chemical Society of Japan "Handbook of Chemistry: Pure Chemistry II, 5th ed.", Maruzen Publishing, Tokyo (2004) pp. 629–638.